

# Rotational Analyses for Selected Bands of the $2^1\Sigma_u^+ \leftarrow X^1\Sigma_g^+$ Transition of $\text{Cl}_2^\dagger$

P. Wang,<sup>‡</sup> S. S. Dimov,<sup>§</sup> and R. H. Lipson\*

Department of Chemistry, University of Western Ontario, London, Ontario N6A 5B7, Canada

Received: January 13, 1997; In Final Form: April 15, 1997<sup>⊗</sup>

Rotational analyses are presented for selected bands of the  $2^1\Sigma_u^+ (v'=1-3) \leftarrow X^1\Sigma_g^+ (v''=0)$  transition of supersonically cooled  $\text{Cl}_2$ , recorded in fluorescence excitation near  $\lambda \leq 128$  nm with a tunable, coherent, and monochromatic vacuum ultraviolet laser generated by four-wave difference mixing in Kr gas. Absolute  $J$ -numbering was established in part by spectral simulation. Although the band system is perturbed, the effective rotational constants derived in this work are consistent with theoretical calculations that place the excited two-state equilibrium bond length at  $\sim 2.1$  Å.

## 1. Introduction

Landmark theoretical calculations by Peyerimhoff and Buenker on the electronic structure of  $\text{Cl}_2$  showed that the  $1^1\Sigma_u^+$  states that lie in the vacuum ultraviolet (VUV,  $100 \text{ nm} \leq \lambda \leq 200 \text{ nm}$ ) between  $\sim 145$  and  $125 \text{ nm}$  are subject to strong homogeneous perturbations.<sup>1</sup> The dominant interaction between the diabatic  $4p\pi$  Rydberg state and the third tier ion-pair state that dissociates to  $\text{Cl}^+(^1D_g) + \text{Cl}^-(^1S_g)$  yields a lower energy adiabatic level (called  $1^1\Sigma_u^+$ ), which has a double-well potential energy curve. This structure has now been satisfactorily characterized by several single-photon synchrotron<sup>2-4</sup> and VUV laser studies.<sup>5-7</sup>

For many years, however, the spectroscopy of the higher energy adiabatic  $2^1\Sigma_u^+$  state resulting from the avoided crossing described above was much more poorly understood even though Douglas first reported rough VUV absorption wave numbers for the 2-X transition as early as 1981.<sup>8</sup> Recently, this situation has been reversed through a judicious combination of theory<sup>1</sup> and VUV laser experimentation.<sup>9,10</sup>

The inner wing of the two-state potential energy curve is ascribed diabatically to the inner wall of the third tier ion-pair state above, while the outer wing belongs to the  $4p\pi$  Rydberg state. Owing to the curvature of the potential near its minimum, the excited-state vibrational frequency was predicted to be larger than that for a pure Rydberg state ( $\sim 628\text{--}665 \text{ cm}^{-1}$ <sup>6,11,12</sup>), valence state ( $\sim 260 \text{ cm}^{-1}$ <sup>13</sup>), or the ground state ( $\sim 560 \text{ cm}^{-1}$ <sup>14</sup>) of the molecule. New VUV laser/time-of-flight (TOF) mass spectra of the 2-X transition recorded by our group has verified this point.<sup>10</sup> By carefully measuring the vibrational isotope shifts in several  $v'$  levels, we were able to deduce that the lowest energy isotopic features observed near  $78\text{--}125 \text{ cm}^{-1}$  were most likely not due to  $(v',v'') = (0,0)$  transitions, as previously thought, but to  $(v',v'') = (1,0)$  transitions instead. A least-squares fit of the isotopic transition wavenumbers for  $v' \leq 3$  (renumbered) to a mass-reduced Dunham expansion yielded a two-state vibrational frequency,  $\omega_e'$ , and anharmonicity,  $\omega_e x_e'$ , of  $760.2(22.3)$  and  $-41.5(4.5) \text{ cm}^{-1}$ , respectively. The negative

value of the latter parameter is attributed to local perturbations with, as yet, unidentified electronic state(s).

The 2-X transitions involving excited-state vibrational levels up to  $v' \leq 16$  (renumbered) have also been mapped out in low resolution using synchrotron radiation.<sup>15</sup> The unusual non-Franck-Condon intensity distribution observed for the band system indicates that the electronic transition moment varies as a function of bond length as the upper state changes from valence to Rydberg-like character.<sup>1</sup> Furthermore,  $2^1\Sigma_u^+$  also has a double-well potential energy curve like the 1-state due to an additional avoided crossing at longer bond lengths ( $\sim 2.4$  Å) with the fourth tier ion-pair state that dissociates to  $\text{Cl}^+(^1S_g) + \text{Cl}^-(^1S_g)$ <sup>1</sup>.

The equilibrium bond length,  $r_e'$ , of the 2-state is calculated to be  $r_e' \approx 2.1$  Å, which corresponds roughly to the  $r$  value of the top of the barrier separating the Rydberg and ion-pair portions of the 1-state.<sup>1,2</sup> However, to the best of our knowledge, no rotational analyses for the 2-X transition have ever been reported that can confirm this prediction. For this paper therefore, we have rotationally analyzed our published  $\text{Cl}_2$  2-X VUV laser fluorescence excitation spectra, which were obtained using tunable, coherent, and monochromatic radiation generated by four-wave difference mixing in Kr gas.<sup>16</sup>

## 2. Experimental Section

The experimental apparatus and operating conditions used to record VUV fluorescence excitation spectra of the 2-X transition of jet-cooled  $\text{Cl}_2$  are detailed in refs 10 and 17. In each of the three wavelength regions corresponding to  $2^1\Sigma_u^+ (v' = 1, 2, \text{ and } 3) \leftarrow X^1\Sigma_g^+ (v'' = 0)$ , corrections to the Kr two-photon resonance frequency<sup>18</sup> used to calculate transition wavenumbers in the VUV, required because of phase-matching, were deduced by comparing separate VUV laser spectra of  $\text{CO } A^1\Pi (v' = 10, 11, \text{ and } 12) \leftarrow X^1\Sigma^+ (v'' = 0)$ , respectively, with those in the literature.<sup>19</sup> In this way a generated VUV line width of  $\Delta\nu \approx 0.7 \text{ cm}^{-1}$  could also be estimated from individual rotational lines resolved in the CO spectra. This result establishes the spectral resolving power of the instrument,  $\nu/\Delta\nu$ , to be  $>111, 600$  for  $\lambda < 128 \text{ nm}$ .

## 3. Spectral Results and Analysis

The VUV fluorescence excitation spectrum in the vicinity of the 2-X (1,0) band assigned to the  $^{35}\text{Cl}_2$  isotopomer is reproduced in Figure 1a. The identity of the molecular carrier was established previously using VUV laser/TOF mass spectrometry.<sup>10</sup>

<sup>†</sup> Publication 533 from the Photochemistry Unit, The University of Western Ontario.

<sup>‡</sup> Present address: Gas-Phase Chemical Dynamics Group, Chemistry Division, Argonne National Laboratory, 9700 South Cass Avenue, Argonne, Illinois 60439.

<sup>§</sup> Present address: Advanced Minerals Technology Laboratory, U.W.O. Research Park, 100 Collip Circle, London, Ontario N6G 4X8, Canada.

\* To whom correspondence should be addressed. E-mail: rlipson@uwoxax.uwo.ca.

<sup>⊗</sup> Abstract published in *Advance ACS Abstracts*, May 15, 1997.

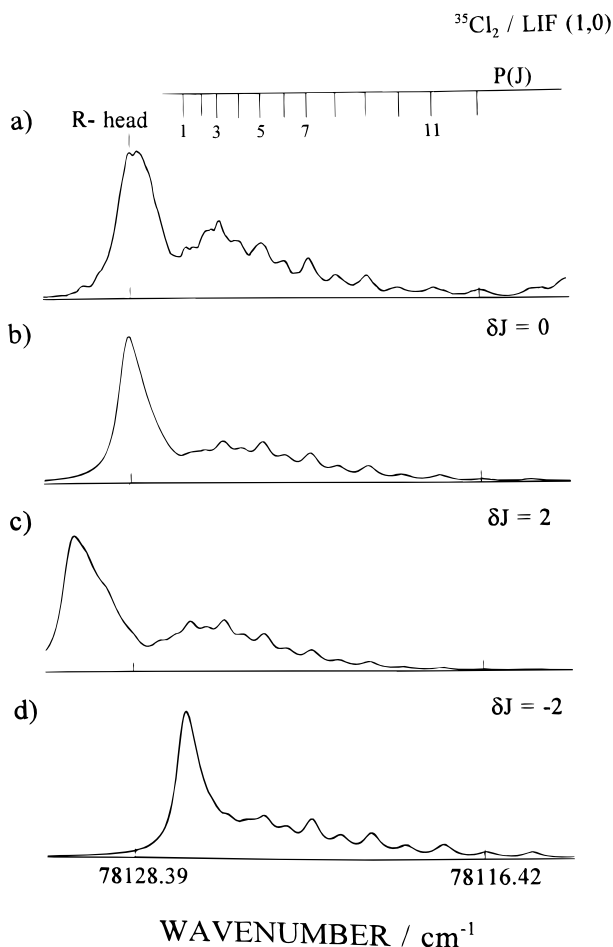


**Figure 1.** (a) Small portion of the vacuum ultraviolet (VUV) laser-excited fluorescence excitation spectrum assigned to the  $2^1\Sigma_u^+$  ( $v' = 1$ )  $\leftarrow$   $X^1\Sigma_g^+$  ( $v'' = 0$ ) transition of  $^{35}\text{Cl}_2$ . (b) Best simulation,  $\delta J = 0$ . (c) Simulation obtained by changing the best set  $\{J\}$  in the P branch by  $\delta J = +2$ . (d) Simulation obtained by changing the best set  $\{J\}$  in the P branch by  $\delta J = -2$ .

The analysis proceeded under the following two assumptions. The first was that the symmetry of the excited state is indeed  $^1\Sigma_u^+$  in agreement with theoretical expectations.<sup>1</sup> Then two branches are expected, R( $J$ ) and P( $J$ ), due to the rotational selection rule  $\Delta J = \pm 1$ .<sup>20</sup> In Figure 1a the higher energy R branch is unresolved while rotational structure can be discerned in the lower energy P branch.

The second assumption was that the vibronic band assignments in ref 10 for the 2-X band system are correct. Although we are confident about the (1,0) isotopic transitions, the possibility of state misidentification is much larger in the region of the (2,0) and (3,0) bands where more complex vibrational structure was observed.

The intensity alternation clearly evident in the P branch shown in Figure 1a arises for  $^{35}\text{Cl}_2$  because the nuclear spin,  $I$ , of atomic  $^{35}\text{Cl}$  is  $3/2$ .<sup>21</sup> Consequently, transitions originating from odd  $J$  rotational levels are expected to be stronger than those from even  $J$  levels by a ratio of 5:3.<sup>20</sup> However, because of the unresolved R branch, absolute  $J$ -numbering could not be established by ground-state combination differences. Still, there are only a few lines in the spectrum due to the low internal rotational temperature of the molecular sample, and therefore, because of the intensity alternation described above, a reasonable  $J$  numbering could be deduced almost by inspection to within  $\pm 2$ . For a given set of rotational assignments, the averaged transition wavenumbers of the P( $J$ ) lines,  $\nu_i$ , were fitted by the method of least-squares to a Dunham expansion of the form

$$\nu_i = \nu_0 + \sum_n Y'_{0,n} [J(J+1)]^n - \sum_m Y''_{0,m} [J''(J''+1)]^m \quad (1)$$

where  $\nu_0$  is the band origin of the particular rovibronic transition,  $\{Y'_{0,n}\}$  is the set of two-state  $v'$  rotational Dunham constants, and  $\{Y''_{0,m}\}$  are the  $v'' = 0$  ground-state rotational parameters, which, for our analyses, were constrained to their known values.<sup>14</sup>

The final rotational assignments and excited-state constants were confirmed by computer simulation of the observed spectrum. The calculation began by estimating the rotational temperature,  $T_{\text{rot}}$ , in the supersonic jet. The maximum rotational population in  $v'' = 0$  was then expected to reside in level  $J''_{\text{max}}$ , where  $J''_{\text{max}}$  is the integer quantum number closest to that obtained from eq 2, which is derived from a Boltzmann distribution function.<sup>20</sup>

$$J''_{\text{max}} = [k_B T_{\text{rot}} / (2B_0'')]^{1/2} - 1/2 \quad (2)$$

Here,  $k_B$  and  $B_0''$  are the Boltzmann constant and the rotational  $B$  value for  $v'' = 0$ , respectively. P( $J$ ) and R( $J$ ) line transition wavenumbers were then calculated for  $J''$  values up to  $10J''_{\text{max}}$  using the two-state rotational constants derived from the least-squares fit of the experimental data.

Each P( $J$ ) and R( $J$ ) line, centered at its own frequency,  $\nu_i$ , was digitally broadened (typically with  $\geq 100$  points) over a specified frequency range corresponding to the whole band in question using a normalized Lorentzian line shape function with an estimated full width at half-maximum,  $\Delta\nu$ . A Lorentzian function was chosen because the band system is partially predissociated. However, there appeared to be little difference between these simulations and a few others performed using Gaussian line shape functions. Each Lorentzian was multiplied by the appropriate Boltzmann and Hönl–London factors,<sup>20</sup> an intensity alternation factor (5 for odd  $J''$ ; 3 for even  $J''$ ) for the specified  $J''$  level involved in the transition, and then coadded to yield the simulated spectrum.

Initially, the inputted values of the spectral line width and the rotational temperature were varied until the best simulation of the spectrum in Figure 1a was achieved ( $\Delta\nu \approx 0.7 \text{ cm}^{-1}$  and  $T_{\text{rot}} \approx 15 \text{ K}$ ). These parameters were subsequently fixed for all other calculations. Interestingly, the value of  $\Delta\nu$  derived from this procedure agrees with that measured from the VUV laser CO spectra and indicates that the frequency resolution of the  $\text{Cl}_2$  data is essentially determined by the instrument. Still, since the 2-state is also known to be partially predissociated,<sup>10,15</sup> it can be concluded, therefore, that this rate is not fast enough to make a measurable contribution to the rotational line width under our experimental conditions. The line width used, however, does lead to a lower limit for the excited-state predissociation lifetime of  $>7.6 \text{ ps}$ .

In the end, the best  $J$ -numbering used to determine the molecular constants was that which produced a minimum least-squares fit standard deviation,  $\sigma$ , and the best simulation. The latter can be inspected in Figure 1b. Both the frequency position of the R branch band head and the individual lines of the P branch are well reproduced. We contend that the  $J$ -numbering is firm because the simulations obtained by changing the absolute  $J$ -numbering of the P branch by  $\delta J = +2$  (Figure 1c) or  $\delta J = -2$  (Figure 1d) (as required by the intensity alternation) are in much poorer agreement with the experimental observation. Here, it should be appreciated that the different simulations were carried out over the exact same frequency range as the observed spectrum but using new band origins and rotational  $B'_v$  constants derived from least-squares fits of the reassigned  $J$  lines to eq 1. Consequently, a  $J$ -numbering was not considered acceptable if

**TABLE 1: Rotational Assignments and Transition Wavenumbers (cm<sup>-1</sup>) for the P Branches, and the Calculated R Band Heads for the Three Isotopic 2<sup>1</sup>Σ<sub>u</sub><sup>+</sup> (v' = 1) ← X<sup>1</sup>Σ<sub>g</sub><sup>+</sup> (v'' = 0) Transitions of Cl<sub>2</sub>**

J	<sup>35</sup> Cl <sub>2</sub>		<sup>35</sup> Cl <sup>37</sup> Cl		<sup>37</sup> Cl <sub>2</sub>	
	P(J)	R(J)	P(J)	R(J)	P(J)	R(J)
1	78 126.09(-2) <sup>a</sup>					
2	78 125.63(5)		78 110.81(9)	78112.44 <sup>b</sup>		
3	78 125.00(0)		78 110.01(3)		78 091.75(10)	78 094.3 <sup>b</sup>
4	78 124.38(3)		78 109.12(-1)		78 090.90(-5)	
5	78 123.60(-4)		78 108.03(-11)		78 090.16(0)	
6	78 122.85(-2)	78 128.39 <sup>b</sup>	78 106.99(-8)		78 089.12(-12)	
7	78 121.99(-4)		78 105.89(-3)		78 088.15(-1)	
8	78 121.11(3)		78 104.73(2)		78 086.91(0)	
9	78 120.03(-1)		78 103.56(9)		78 085.63(20)	
10	78 118.90(1)		78 102.29(8)		78 083.57(-12)	
11	78 117.65(6)		78 100.91(-8)		78 081.65(1)	
12	78 116.10(-4)					

<sup>a</sup> Observed and calculated residuals in units of 10<sup>-2</sup> cm<sup>-1</sup>. <sup>b</sup> Predicted J value associated with the calculated R head.

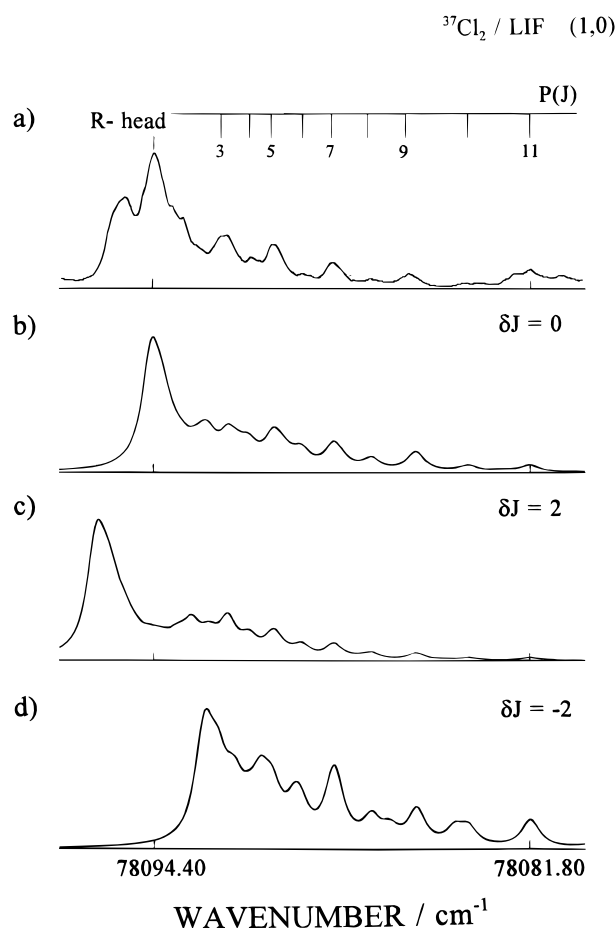


**Figure 2.** (a) Small portion of the VUV laser-excited fluorescence excitation spectrum assigned to the 2<sup>1</sup>Σ<sub>u</sub><sup>+</sup> (v' = 1) ← X<sup>1</sup>Σ<sub>g</sub><sup>+</sup> (v'' = 0) transition of <sup>37</sup>Cl<sub>2</sub>. The feature just to the blue of the R head is currently unassigned. (b) Best simulation, δJ = 0. (c) Simulation obtained by changing the best set {J} in the P branch by δJ = +2. (d) Simulation obtained by changing the best set {J} in the P branch by δJ = -2.

the resultant simulation could only match the observed spectrum by frequency shifting it wholesale to do so.

The VUV fluorescence excitation spectrum of the 2-X transition of <sup>37</sup>Cl<sub>2</sub>(1,0) band of the 2-X transition is shown in Figure 2 a. Like <sup>35</sup>Cl, atomic <sup>37</sup>Cl also has a nuclear spin of I = 3/2.<sup>21</sup> Consequently, the homonuclear <sup>37</sup>Cl<sub>2</sub> molecule exhibits the same intensity alternation as <sup>35</sup>Cl<sub>2</sub>. The best simulation is shown in Figure 2b, while those resulting from a change in the best J-numbering by δJ = ±2 can be examined in parts c and d of Figure 2. At this time the feature to the blue of the R head is unassigned.

The fluorescence excitation spectrum of the 2-X (1,0) band

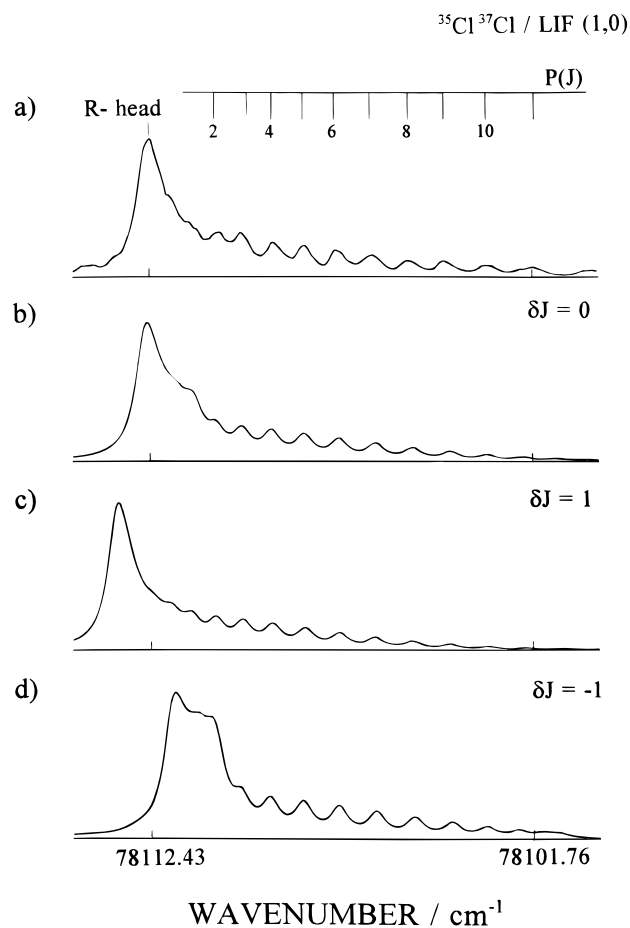


**Figure 3.** (a) Small portion of the VUV laser-excited fluorescence excitation spectrum assigned to the 2<sup>1</sup>Σ<sub>u</sub><sup>+</sup> (v' = 1) ← X<sup>1</sup>Σ<sub>g</sub><sup>+</sup> (v'' = 0) transition of <sup>35</sup>Cl<sup>37</sup>Cl. (b) Best simulation, δJ = 0. (c) Simulation obtained by changing the best set {J} in the P branch by δJ = +1. (d) Simulation obtained by changing the best set {J} in the P branch by δJ = -1.

of <sup>35</sup>Cl<sup>37</sup>Cl (Figure 3a) differs from the other Cl<sub>2</sub> isotopomers in that an intensity alternation was neither expected nor observed for this heteronuclear molecule. Consequently, the simulation was carried out exactly as described above but without including the intensity alternation factor. The best result (Figure 3b) reproduces the experimental data well, while those where the absolute J-numbering in the P branch was changed by δJ = ±1 (parts c and d of Figure 3) do not. All transition wavenumbers and rotational assignments for the three isotopic bands are provided in Table 1, while the excited state rotational constants can be found in Table 2.

**TABLE 2: Rotational Constants (cm<sup>-1</sup>) for the Isotopic Bands of the 2<sup>1</sup>Σ<sub>u</sub><sup>+</sup> (v' = 1–3) ← X<sup>1</sup>Σ<sub>g</sub><sup>+</sup> (v'' = 0) Transitions of Cl<sub>2</sub>**

parameter (cm <sup>-1</sup> )	<sup>35</sup> Cl <sub>2</sub>	<sup>35</sup> Cl <sup>37</sup> Cl	<sup>37</sup> Cl <sub>2</sub>
(v',v'') = (1,0)			
Y <sub>0,0</sub> (~ν <sub>0</sub> )	78126.604(21) <sup>a</sup>	78111.800(59)	78093.25(10)
Y <sub>0,1</sub> (~B' <sub>v</sub> )	0.21881(95)	0.1696(29)	0.1955(46)
-10 <sup>3</sup> Y <sub>0,2</sub> (~D' <sub>v</sub> )	0.0790(75)	-0.148(26)	0.224(39)
r' <sub>v</sub> <sup>b</sup>	2.0991(46)	2.352(20)	2.160(25)
σ <sup>c</sup>	0.04	0.09	0.12
(v',v'') = (2,0)			
Y <sub>0,0</sub> (~ν <sub>0</sub> )	79052.09(19)	79023.37(13)	78993.868(43)
Y <sub>0,1</sub> (~B' <sub>v</sub> )	0.166(10)	0.1088(27)	0.2114(23)
-10 <sup>3</sup> Y <sub>0,2</sub> (~D' <sub>v</sub> )	0.43(10)	d	0.542(21)
r' <sub>v</sub>	2.410(72)	2.936(36)	2.077(11)
σ	0.19	0.21	0.08
(v',v'') = (3,0)			
Y <sub>0,0</sub> (~ν <sub>0</sub> )	80053.990(43)	80014.191(42)	79982.23(14)
Y <sub>0,1</sub> (~B' <sub>v</sub> )	0.1874(13)	0.1556(15)	0.1375(63)
-10 <sup>3</sup> Y <sub>0,2</sub> (~D' <sub>v</sub> )	0.0508(74)	-0.2973(96)	0.115(49)
r' <sub>v</sub>	2.2682(79)	2.455(12)	2.576(59)
σ	0.08	0.08	0.26

<sup>a</sup> 1σ standard errors. <sup>b</sup> Bond length in angstrom units. <sup>c</sup> Standard deviation of the least-squares fit. <sup>d</sup> Parameter not determined statistically.

The simulations for the isotopic bands making up the 2-X (2,0) and (3,0) transitions are of comparable quality to those presented in Figures 1–3.<sup>22</sup> Their transition wavenumbers are cataloged in Tables 3 and 4, respectively, while the molecular

constants obtained from fitting the data to a Dunham expansion are also listed in Table 2.

#### 4. Discussion and Conclusions

The main result of this paper is the first rotational constants for the 2-X transition from resolved spectra. It should be appreciated, however, that the constants must be viewed as effective because the band system is perturbed. In particular, the variation of the B'<sub>v</sub> values with v' is irregular, with perhaps the most anomalous constants being those associated with v' = 2. Consequently, no attempt was made to determine α<sub>e</sub> (≈ -Y<sub>1,1</sub>) and an equilibrium B'<sub>e</sub> value by fitting the B'<sub>v</sub>'s together. Nevertheless, the range of bond lengths listed in Table 2 (2.93 Å ≥ r'<sub>v</sub> ≥ 2.08 Å), while large, appears to be consistent with theoretical calculations, which place the two-state minimum at ~2.1 Å.<sup>1</sup>

As noted before, the 2-X transitions with v' ≥ 2 are not simple triplets in fluorescence excitation like (v',v'') = (1,0) but are more complex because of perturbations.<sup>9,10</sup> The electronic level(s) perturbing the 2-state, however, have not been unambiguously identified. All the unassigned vibronic transitions are red-shaded, and in certain instances, the band intensities are quite appreciable. Preliminary rotational analyses have now been completed for several of the stronger <sup>35</sup>Cl<sub>2</sub> features in the vicinity of 2<sup>1</sup>Σ<sub>u</sub><sup>+</sup> (v' = 1,2) ← X<sup>1</sup>Σ<sub>g</sub><sup>+</sup> (v'' = 0).<sup>22</sup> The resultant B'<sub>v</sub>'s for these transitions range from ~0.06 to 0.18 cm<sup>-1</sup>, which lie closer in value to those expected for high-lying levels of an ion-pair perturber than low v' levels of an isoenergetic Rydberg state. More effort will be required to deperturb the spectrum and to

**TABLE 3: Rotational Assignments and Transition Wavenumbers (cm<sup>-1</sup>) for the P Branches, and the Calculated R Band Heads for the Three Isotopic 2<sup>1</sup>Σ<sub>u</sub><sup>+</sup> (v' = 2) ← X<sup>1</sup>Σ<sub>g</sub><sup>+</sup> (v'' = 0) Transitions of Cl<sub>2</sub>**

J	<sup>35</sup> Cl <sub>2</sub>		<sup>35</sup> Cl <sup>37</sup> Cl		<sup>37</sup> Cl <sub>2</sub>	
	P(J)	R(J)	P(J)	R(J)	P(J)	R(J)
0				79 023.6 <sup>b</sup>		
1		79 052.6 <sup>b</sup>				
2						
3	79 050.20(5) <sup>a</sup>		79 021.09(-9)		78 992.34(4)	78 995.12 <sup>b</sup>
4	79 049.16(1)		79 019.65(-29)		78 991.80(-1)	
5	79 047.91(-3)		79 018.67(23)		78 990.87(-1)	
6	79 046.37(-9)		79 016.94(26)		78 989.97(8)	
7	79 044.55(-12)		79 014.77(9)		78 988.92(2)	
8	79 042.86(35)		79 012.35(-6)		78 987.47(4)	
9	79 039.70(-19)		79 009.69(-20)		78 985.65(10)	
10	79 036.78(2)		79 007.17(6)		78 983.07(-10)	
11					78 980.18(2)	

<sup>a</sup> Observed and calculated residuals in units of 10<sup>-2</sup> cm<sup>-1</sup>. <sup>b</sup> Predicted J value associated with the calculated R head.

**TABLE 4: Rotational Assignments and Transition Wavenumbers (cm<sup>-1</sup>) for the P Branches, and the Calculated R Bandheads for the Three Isotopic 2<sup>1</sup>Σ<sub>u</sub><sup>+</sup> (v' = 3) ← X<sup>1</sup>Σ<sub>g</sub><sup>+</sup> (v'' = 0) Transitions of Cl<sub>2</sub>**

J	<sup>35</sup> Cl <sub>2</sub>		<sup>35</sup> Cl <sup>37</sup> Cl		<sup>37</sup> Cl <sub>2</sub>	
	P(J)	R(J)	P(J)	R(J)	P(J)	R(J)
1	80 053.63(12) <sup>a</sup>			80 014.85 <sup>b</sup>	79 982.08(31)	79 982.6 <sup>b</sup>
2	80 083.24(33)		80 013.41(12)		79 981.11(-1)	
3	80 052.14(-6)	80 054.80 <sup>b</sup>	80 012.39(-10)		79 979.97(-32)	
4	80 051.38(2)		80 011.46(-3)		79 978.95(-31)	
5	80 050.41(-1)		80 010.32(4)		79 978.06(4)	
6	80 049.31(-4)		80 008.84(-2)		79 976.81(22)	
7	80 048.09(-5)		80 007.08(-7)		79 975.15(25)	
8	80 046.75(-5)		80 005.13(0)		79 973.20(21)	
9	80 045.22(-9)		80 002.78(4)		79 970.41(-40)	
10	80 043.74(7)		79 999.96(2)		79 968.28(-6)	
11	80 041.87(1)		79 996.63(-3)		79 965.61(4)	
12	80 039.99(12)		79 992.89(8)		79 962.51(5)	
13	80 037.75(3)		79 988.29(-5)			
14	80 035.22(-8)					

<sup>a</sup> Observed and calculated residuals in units of 10<sup>-2</sup> cm<sup>-1</sup>. <sup>b</sup> Predicted J value associated with the calculated R head.

completely eliminate the possibility that in the region of  $(v',v'') = (2,0)$  and  $(3,0)$  2-state misassignments are not responsible for the spread in  $r'_v$  values found in Table 2.

In our experiment, rotationally resolved excitation spectra were also obtained by monitoring Cl<sub>2</sub><sup>+</sup> produced by  $(1 + 1')$  resonance-enhanced multiphoton ionization (REMPI) in time-of-flight at the same time as VUV fluorescence from the jet.<sup>10</sup> The unusual rotational line intensity distributions found were credited qualitatively to an additional resonance enhancement at the  $(1 + 1')$  energy range due to a superexcited state.<sup>23</sup>

This appears to contradict the conclusions of Koenders, De Lange, and co-workers<sup>24,25</sup> who obtained a complicated photoelectron spectrum in an earlier REMPI-photoelectron (PE) spectroscopy experiment using  $2^1\Sigma_u^+$  as the intermediate level. They attributed the complexity to the mixed Rydberg-valence character of the 2-state. Removing an electron from the 2-state diabatic Rydberg component produces Cl<sub>2</sub><sup>+</sup> in its X<sup>2</sup>Π<sub>g</sub> ground state, while the diabatic ion-pair state is built upon an excited  $2^2\Sigma_g^+$  ion-core. The presence of both these ionic states in the PE spectrum was thought to arise from simultaneous  $(3 + 1)$  and  $(3 + 2)$  multiphoton ionizations.

Recently, we added a PE spectrometer to our experimental system.<sup>26</sup> We can also restrict the photon excitation to  $(1 + 1')$  VUV-REMPI alone using divergent fundamental laser beams, since this minimizes the possibility of higher order REMPI processes. Experiments are planned for the near future, therefore, to resolve this issue by recording VUV laser-excited Cl<sub>2</sub> 2-state dispersive PE spectra.

**Acknowledgment.** This paper is dedicated to the memory of Dr. S. King Wong. The financial support of the Natural Sciences and Engineering Research Council of Canada (NSERC) is gratefully acknowledged.

## References and Notes

- (1) Peyerimhoff, S. D.; Buenker, R. J. *Chem. Phys.* **1981**, *57*, 279.
- (2) Moeller, T.; Jordan, B.; Gürtler, P.; Zimmerer, G.; Haaks, D.; Le Calvé, J.; Castex, M. C. *Chem. Phys.* **1982**, *76*, 295.
- (3) Moeller, T.; Jordan, B.; Gürtler, P.; Zimmerer, G.; Haaks, D.; LeCalvé, J.; Castex, M. C. *Spectral Line Shapes* **1983**, *2*, 597.
- (4) Wörmer, J.; Möller, T.; Stapelfeldt, J.; Zimmerer, G.; Haaks, D.; Kampf, S.; Le Calvé, J.; Castex, M. C. *Z. Phys. D* **1988**, *7*, 383.
- (5) Yamanouchi, K.; Tsuchizawa, T.; Miyawaki, J.; Tsuchiya, S. *Chem. Phys. Lett.* **1989**, *156*, 301.
- (6) Tsuchizawa, T.; Yamanouchi, Y.; Tsuchiya, S. *J. Chem. Phys.* **1990**, *93*, 111.
- (7) Wang, P.; Okuda, I. V.; Dimov, S. S.; Lipson, R. H. *Chem. Phys. Lett.* **1994**, *229*, 370.
- (8) Douglas, A. E. *Can. J. Phys.* **1981**, *59*, 835.
- (9) Tsukiyama, K.; Kurematsu, Y.; Tsukakoshi, M.; Misu, A.; Kasuya, T. *Chem. Phys. Lett.* **1988**, *152*, 523.
- (10) Wang, P.; Dimov, S. S.; Rosenblood, G.; Lipson, R. H. *J. Phys. Chem.* **1995**, *99*, 3984.
- (11) Zafirooulos, V.; Fu, G. S.; Hontzopoulos, E.; Fotakis, C.; Castex, M. C. *Chem. Phys. Lett.* **1991**, *179*, 258.
- (12) Jóhannesson, G. H.; Wang, H.; Kvaran, A. *J. Mol. Spectrosc.* **1996**, *179*, 334.
- (13) Clyne, M. A. A.; Coxon, J. A. *J. Mol. Spectrosc.* **1970**, *33*, 381.
- (14) Douglas, A. E.; Hoy, A. R. *Can. J. Phys.* **1975**, *53*, 1965.
- (15) Lee, L. C.; Suto, M.; Tang, K. Y. *J. Chem. Phys.* **1986**, *84*, 5277.
- (16) Hilber, G.; Lago, A.; Wallenstein, R. *J. Opt. Soc. Am. B* **1987**, *4*, 1753.
- (17) Dimov, S. S.; Lipson, R. H.; Turgeon, T.; Vanstone, J. A.; Wang, P.; Yang, D. S. *J. Chem. Phys.* **1994**, *100*, 8666.
- (18) Kaufman, V.; Humphreys, C. J. *J. Opt. Soc. Am.* **1969**, *59*, 1614.
- (19) Tilford, S. G.; Simmons, J. D. *J. Phys. Chem. Ref. Data* **1972**, *1*, 147.
- (20) Herzberg, G. *Spectra of Diatomic Molecules*; Van Nostrand Reinhold: New York, 1950.
- (21) Radzig, A. A.; Smirnov, B. M. *Reference Data on Atoms, Molecules, and Ions*; Springer-Verlag Series in Chemical Physics 31; Springer-Verlag: Berlin, 1985.
- (22) Wang, P. Ph.D. Thesis, University of Western Ontario, 1996.
- (23) Lefebvre-Brion, H.; Suzor-Weiner, A. *Comments At. Mol. Phys.* **1994**, *29*, 305.
- (24) Koenders, B. G.; Wieringa, D. M.; Drabe, K. E.; De Lange, C. A. *Chem. Phys.* **1987**, *118*, 113.
- (25) Koenders, B. G.; De Lange, C. A. *Comments At. Mol. Phys.* **1990**, *24*, 119.
- (26) Hu, X. K.; Mao, D. M.; Dimov, S. S.; Lipson, R. H. *Phys. Rev. A* **1996**, *54*, 2814.